applied sciences

MDPI

Article

Calcination-Free Biosynthesis of Silica Nanoparticles from Residual Rice Husk Using *Aspergillus niger*

Daniel Escorcia-Díaz [1], Sebastián García-Mora [1], Leidy Rendón-Castrillón [2], Margarita Ramírez-Carmona [2] and Carlos Ocampo-López [2,*]

[1] Nanotechnology Engineering Program, Centro de Estudios y de Investigación en Biotecnología (CIBIOT), Chemical Engineering Faculty, Universidad Pontificia Bolivariana, Medellín 050031, Colombia; daniel.escorcia@upb.edu.co (D.E.-D.); sebastian.garciamo@upb.edu.co (S.G.-M.)

[2] Chemical Engineering Program, Centro de Estudios y de Investigación en Biotecnología (CIBIOT), Chemical Engineering Faculty, Universidad Pontificia Bolivariana, Medellín 050031, Colombia; leidy.rendon@upb.edu.co (L.R.-C.); margarita.ramirez@upb.edu.co (M.R.-C.)

* Correspondence: carlos.ocampo@upb.edu.co

Abstract

In this study, composite silica-containing nanostructures were biosynthesized from residual rice husk through a fermentative process using *Aspergillus niger* at room temperature without calcination. The obtained nanostructures were initially characterized by UV–Vis spectrophotometry, Fourier-transform infrared spectroscopy (FTIR), and field-emission scanning electron microscopy (FE-SEM) to determine their optical and structural properties compared with chemically synthesized silica. The results demonstrated the successful formation of composite silica-containing amorphous nanostructures under ambient conditions without the use of calcination or mineral acids. UV–Vis analysis revealed intense absorption in the deep ultraviolet region, attributed to electronic transitions associated with Si–O–Si bonds within the amorphous silica network. FTIR analysis enabled the identification of functional groups present on the material surface, providing direct evidence of the nanostructures' chemical composition. Additionally, FE-SEM micrographs showed that the rice husk surface after biosynthesis exhibited a rough and porous texture with a morphology consistent with the formation of composite silica-containing amorphous nanostructures, in agreement with the characteristic Si–O–Si vibrational bands observed in the FTIR spectra and the strong ultraviolet absorption detected by UV–Vis analysis.

Keywords: biogenic nanosilica; fungal bioleaching; agroindustrial waste valorization; calcination-free synthesis; sustainable nanomaterial production

Check for updates

Academic Editors: Voltaire Sant'Anna and Lilian Raquel Hickert

Received: 3 March 2026
Revised: 12 April 2026
Accepted: 14 April 2026
Published: 19 April 2026

Copyright: © 2026 by the authors. Licensee MDPI, Basel, Switzerland. This article is an open access article distributed under the terms and conditions of the Creative Commons Attribution (CC BY) license.

1. Introduction

Silica nanoparticles have become key materials in modern nanotechnology due to their high surface area, chemical stability, and versatile optical properties [1]. In their amorphous or nanostructured forms, silica particles (SiO_2) exhibit outstanding functionality in fields such as photonics, catalysis, the pharmaceutical industry, environmental remediation, and smart coatings [2,3]. Their widespread application in dielectric devices, controlled drug delivery systems, and advanced composite materials has intensified interest in developing sustainable and cost-effective production routes [4].

Rice husk, a byproduct of the rice milling process, is generated in large volumes worldwide and represents an abundant and underutilized source of silica [5]. More than 750 million tons of rice are harvested annually worldwide, generating approximately

137 million tons of husk [5]. This residue contains 15–20 wt% silica, primarily in amorphous form and localized within the epidermal tissues of the husk. However, its improper disposal, such as uncontrolled burning, results in environmental pollution and energy losses [2].

Conventional methods for silica production rely on thermal and acid treatments, which are energy-intensive and environmentally hazardous. Processes such as sol–gel synthesis or alkaline extraction from ash require calcination at temperatures above 600 °C, extraction with strong acids (HCl or H_2SO_4), and extended post-treatment steps to remove carbon residues or metallic impurities [1,3]. Although these methodologies enable the production of high-purity silica with surface areas of up to 409 m^2/g, they involve corrosive reagents, generate acidic effluents, and pose significant operational risks [5].

In this context, biosynthesis has emerged as a sustainable alternative for the extraction of valuable compounds from residual solid substrates by harnessing microbial metabolism as the driving force [6]. Several fungal species, such as *Fusarium oxysporum* and *Aspergillus niger*, have demonstrated the ability to solubilize siliceous materials through the secretion of organic acids and extracellular proteins [7,8]. These systems operate under moderate conditions, including room temperature, near-neutral pH, and without the addition of chemical reagents, enabling the production of silica nanoparticles in the 2–10 nm range [2,8]. Furthermore, biological processes allow for the simultaneous purification and stabilization of silica without the need for calcination or additional chemical modifications [9].

Despite this potential, studies on biosynthesis applied to the production of silica nanoparticles from residual rice husk remain limited, particularly under controlled bioprocessing conditions. Most previous research has focused on rice husk ash (RHA), generated by combustion, a step that partially destroys the organic matrix and requires high energy input [3,5]. In contrast, the present study differs by directly employing native rice husk, both whole and ground, without calcination or thermal treatments, and operating at room temperature (20 °C), thereby reinforcing the eco-efficient and sustainable nature of the process. Moreover, few studies have comprehensively characterized biogenic silica by integrating UV–Vis absorbance spectra, FTIR profiles, surface morphology by microscopy, and functional group analysis, key elements for validating its applicability in advanced systems.

In this context, the present study proposes a biologically mediated route for the synthesis of silica-based nanostructures from residual rice husk using *Aspergillus niger*, avoiding the external addition of strong mineral acids and eliminating the need for high-temperature calcination. Unlike traditional extraction methods, the process relies on microbial metabolic activity, which may generate organic acids in situ, promoting the gradual solubilization of silica under mild conditions. This approach contributes to the valorization of agricultural waste while exploring sustainable alternatives for silica recovery. Therefore, this work aims to provide insights into environmentally friendly pathways within the framework of green nanotechnology and circular bioeconomy. In addition, the physicochemical properties of the obtained materials are evaluated to assess their structural characteristics and potential applicability.

2. Materials and Methods

2.1. Rice Husk

The rice husk used in this study was obtained from two sources: a commercial rice husk (CRH) distributed for agricultural purposes and husk collected from a field in the La Mojana region, Sucre, Colombia. The latter was used in two forms based on its physical characteristics: whole (WM) and ground (GM) using a disc mill.

The particle size distribution of the ground rice husk was determined by dry sieve granulometric analysis. A set of standard sieves with openings of 1.19 mm, 0.595 mm, 0.297 mm, 0.149 mm, 0.074 mm, and 0.063 mm was used in accordance with ASTM E11-17 [10]. Approximately 400 g of dry sample were placed in the sieve column and subjected to mechanical agitation for 10 min using a Ro-Tap shaker (W.S. Tyler, Model RX-29, Mentor, OH, USA). After separation, the mass retained in each fraction was recorded to calculate the percentage retained, cumulative percentage retained, and percentage passing. These values were used to construct the particle size distribution curve, which served as a reference for the physical characterization of the substrate.

2.2. Microorganism

The microorganism used for biosynthesis was *Aspergillus niger*, obtained from the strain collection of the Centro de Estudios y de Investigación en Biotecnología (CIBIOT) and maintained in the laboratory on potato dextrose agar (PDA) in Petri dishes. Incubation was carried out at room temperature (22–25 °C) for 7 days.

2.3. Biosynthesis of Silica from Rice Husk

Biosynthesis experiments were conducted by fermentation with a working volume of 2 L, establishing a pulp density of 1% *w*/*v* rice husk (mass of husk/total fermentation volume). Three fermentations were performed, each using a different type of husk: CRH, WM, and GM, with their respective replicates.

Prior to each experiment, the reactor was subjected to a sanitization procedure using 10% sodium hypochlorite. The culture medium used for the fermentation of Aspergillus niger is shown in Table 1.

Table 1. Culture medium used for the biosynthesis experiments. The values were adapted from previous studies [11,12].

Source	Concentration (g/L)	Source	Concentration (g/L)
Sucrose	140	$CuSO_4$	4.00×10^{-4}
$(NH_4)_2SO_4$	2.5	$MnSO_4$	1.50×10^{-4}
KH_2PO_4	0.5	NaCl	6
$MgSO_4 \cdot 7H_2O$	0.25	$NaNO_3$	1.5
$ZnSO_4 \cdot 7H_2O$	2.50×10^{-4}	$FeSO_4 \cdot 7H_2O$	2.50×10^{-4}

For the inoculum, a spore suspension of *Aspergillus niger* was prepared by washing the surface of four Petri dishes with 20 mL of sterile water to obtain a homogeneous suspension, which was immediately incorporated into the culture medium in the reactor.

Fermentation kinetics were monitored by measuring pH and soluble silica concentration. Samples were collected every 24 h for 11 days. The pH was measured directly in the extracted aliquots, while silica concentration was determined using the standard colorimetric method ASTM D859-16. This procedure is based on the reaction of the molybdate ion with soluble silica to form a yellow-green complex, which is subsequently reduced with 1-amino-2-naphthol-4-sulfonic acid to generate a blue complex [13].

For quantification, a calibration curve was prepared in the range of 0.1 to 5 mg/L of silica, recording absorbance at 640 nm using a UV–Vis spectrophotometer (Shimadzu UV-1606 PC, Kyoto, Japan). Samples obtained during biosynthesis were filtered and diluted to fall within this concentration range, and their absorbance values were interpolated on the calibration curve to determine the silica content.

Based on the silica concentration results from the biosynthesis experiments, the nanoparticles produced using commercial rice husk (CRH) were characterized using the sample collected on day 11, corresponding to the end of the fermentation process.

2.4. Characterization of Silica Nanoparticles

The nanoparticles obtained through biosynthesis were characterized using spectroscopic techniques and electron microscopy to evaluate their optical, chemical, and morphological properties.

2.4.1. UV–Vis Spectroscopy

At the end of the biosynthesis process, a 10 mL liquid sample of the supernatant was collected. The sample was filtered through a 0.45 µm membrane filter (Millipore, Burlington, MA, USA) to remove solid residues. A spectral scan was then performed using a UV–Vis spectrophotometer (Shimadzu UV-1606 PC, Kyoto, Japan) in the range of 200 to 700 nm, with particular attention to the 230–400 nm region, where the main absorption bands of silica nanoparticles have been reported [14–16].

Based on the UV–Vis spectrum, the optical band gap of the silica nanoparticles was estimated using Equation (1):

$$E_g = \frac{hc}{\lambda_{onset}} \quad (1)$$

where

E_g is the band gap energy in electronvolts (eV);
λ_{onset} is the wavelength (nm) at which significant absorption begins in the UV–Vis spectrum;
hc is the product of Planck's constant and the speed of light, equal to 1240 eV·nm.

2.4.2. Fourier-Transform Infrared Spectroscopy (FTIR)

The infrared spectrum was obtained using a Nicolet 6700 spectrometer (Thermo Fisher Scientific, Waltham, MA, USA) equipped with a single-reflection attenuated total reflectance (ATR) accessory and a type IIA diamond crystal mounted on tungsten carbide. Measurements were carried out in the range of 4000 to 400 cm^{-1}, with a resolution of 4 cm^{-1} and a total of 32 scans per sample.

2.4.3. Field-Emission Scanning Electron Microscopy (FE-SEM)

Field-emission scanning electron microscopy (FE-SEM) analysis was performed using a Thermo Scientific Apreo 2s microscope (Thermo Fisher Scientific, Waltham, MA, USA). The rice husk sample was coated with a thin layer of gold and mounted on carbon tape prior to analysis. High-resolution images were acquired to examine the sample morphology and determine the size of the silica particles.

Elemental analysis by energy-dispersive X-ray spectroscopy (EDS) was conducted in three different areas of the sample using the same instrument to identify the elements present.

Morphology and particle size were analyzed using the Thermo Scientific Apreo 2s FE-SEM system (Thermo Fisher Scientific, Waltham, MA, USA). Micrographs were acquired at a magnification of 80,000× and an accelerating voltage of 2.00 kV. Particle size determination was performed through image analysis using ImageJ Fiji software, version 1.54f (National Institutes of Health, Bethesda, MD, USA), evaluating a representative set of particles to generate size distribution histograms.

3. Results and Discussion

3.1. Characterization of Rice Husk Samples

The ground rice husk (GM) sample was subjected to dry sieve granulometric analysis to determine the particle size distribution. The results are presented in Table 2, which includes the nominal sieve opening, retained mass, percentage retained, and cumulative percentage.

Table 2. Particle size distribution of ground rice husk (GM).

ASTM Sieve	Opening (mm)	Retained Mass (g)	Retained (%)	Mean Diameter (mm)
20	1.19	100	25	0.893
35	0.595	95	24	0.446
50	0.297	115	29	0.211
100	0.149	35	9	0.111
200	0.074	15	4	0.069
230	0.063	20	5	0.063
Pan	<0.063	20	5	<0.063
Total	—	400	100	—

Approximately 78% of the total mass was distributed within the 0.297 mm to 1.19 mm range, confirming that the applied milling process predominantly produced coarse fractions. This predominance of larger particles is relevant because the specific surface area of the substrate plays a decisive role in biosynthesis efficiency by controlling the accessibility of extracellular metabolites and fungal hyphae to the plant matrix. Previous studies have indicated that an increase in surface area enhances the rate of silica solubilization; however, it does not necessarily increase total extraction when the internal phases of the material are less reactive or become rapidly depleted [2,8].

The cumulative percentage retained curve (Figure 1a) shows a gradual transition between the coarser and finer fractions, with a relatively narrow dispersion around the median. Linear interpolation was used to determine the D10 and D50 percentiles, yielding values of 0.198 mm and 0.405 mm, respectively. The D50 value, representing the median particle size, indicates that half of the material exhibits a diameter smaller than 0.405 mm, reflecting the simultaneous presence of coarse fractions and a significant proportion of fine particles.

The granulometric profile obtained (Figure 1b) suggests that the milling process used could be optimized depending on the biosynthesis strategy. Although a smaller particle size may promote an accelerated initial release of silica due to increased exposed surface area, excessively fine fractions may compact during fermentation, hindering metabolite diffusion and negatively affecting the process [5]. Therefore, the particle size range obtained in this study represents a potentially favorable balance between accessibility and the maintenance of the structural porosity required for fungal penetration.

3.2. Biosynthesis of Silica from Rice Husk

Figure 2 shows the evolution of pH and soluble silica concentration over 11 days of fermentation with *Aspergillus niger*, using three types of substrates: commercial rice husk (CRH), ground rice husk (GM), and whole rice husk (WM). The solubilization of silica in this process can be attributed to microbial metabolic activity, which leads to the in situ

production of organic acids that act as complexing agents, facilitating silica dissolution under controlled biological conditions.

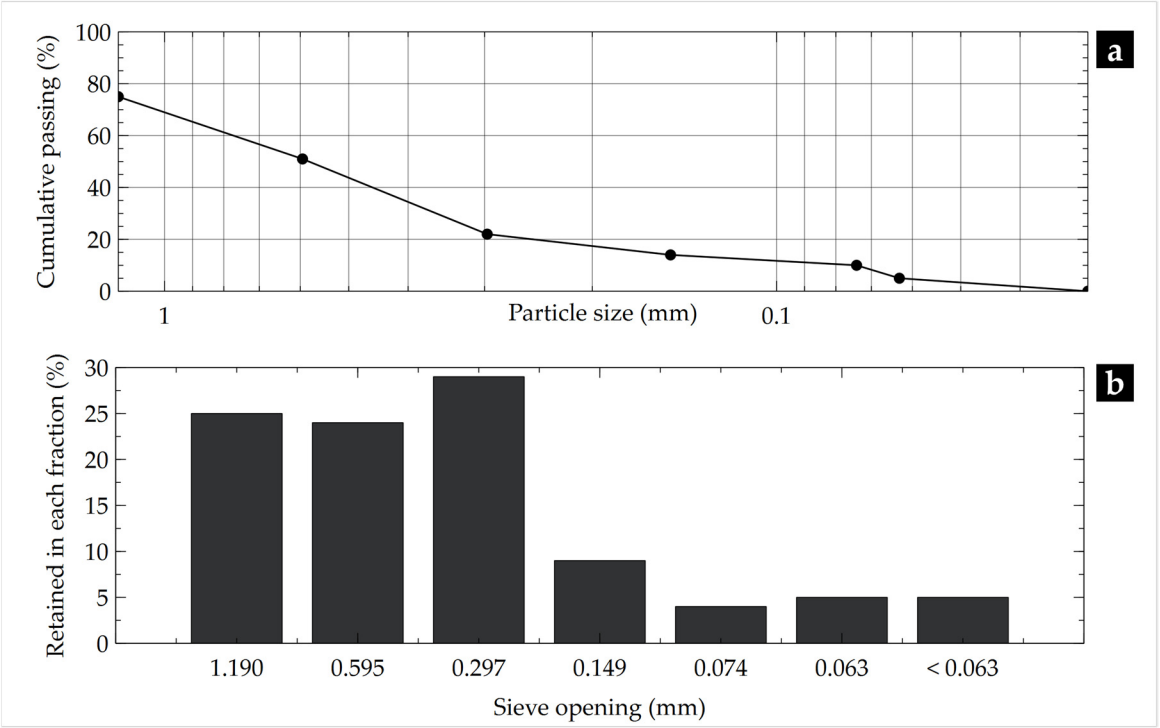


Figure 1. Cumulative particle size distribution curve of ground rice husk obtained by dry sieve analysis in accordance with ASTM E11-17. (**a**) cumulative percentage retained curve; (**b**) retained mass fraction by sieve size (histogram).

The observed decrease in pH during fermentation suggests the progressive production of organic acids as a result of sucrose metabolism by *Aspergillus niger*. This acidification is consistent with the known metabolic pathways of this microorganism, particularly its ability to produce citric acid under carbon-rich conditions. As sucrose is consumed, the accumulation of organic acids contributes to the reduction in pH, which in turn facilitates the solubilization of silica from the rice husk matrix. The temporal evolution of pH and soluble silica concentration indicates a coupled process in which microbial metabolism, acid production, and silica dissolution are closely interrelated.

In the treatment with commercial rice husk (Figure 2a), a progressive decrease in pH was observed from 5.5 to approximately 2.5 by day 6, stabilizing at this value thereafter. Acidification was correlated with a sustained increase in silica concentration, reaching ~52 mg/L (Figure 2) at the end of the experiment. This pattern is consistent with the production of organic acids, mainly oxalic and citric acids, derived from fungal metabolism, which facilitate the dissolution of the amorphous silica present in the husk [17,18].

In the case of ground rice husk (Figure 2b), the pH decreased more rapidly, reaching 2.1 by day 5, indicating a more immediate release of acidifying metabolites, likely promoted by the increased surface area of the substrate. However, the final silica concentration was lower (~30 mg/L) compared to commercial rice husk. This suggests that although mechanical pretreatment accelerates the initial leaching process, the silica reserve available in the fine fractions becomes depleted before the end of fermentation. This behavior has been documented in leaching systems of siliceous materials, where particle size modulates both extraction kinetics and final yield [8].

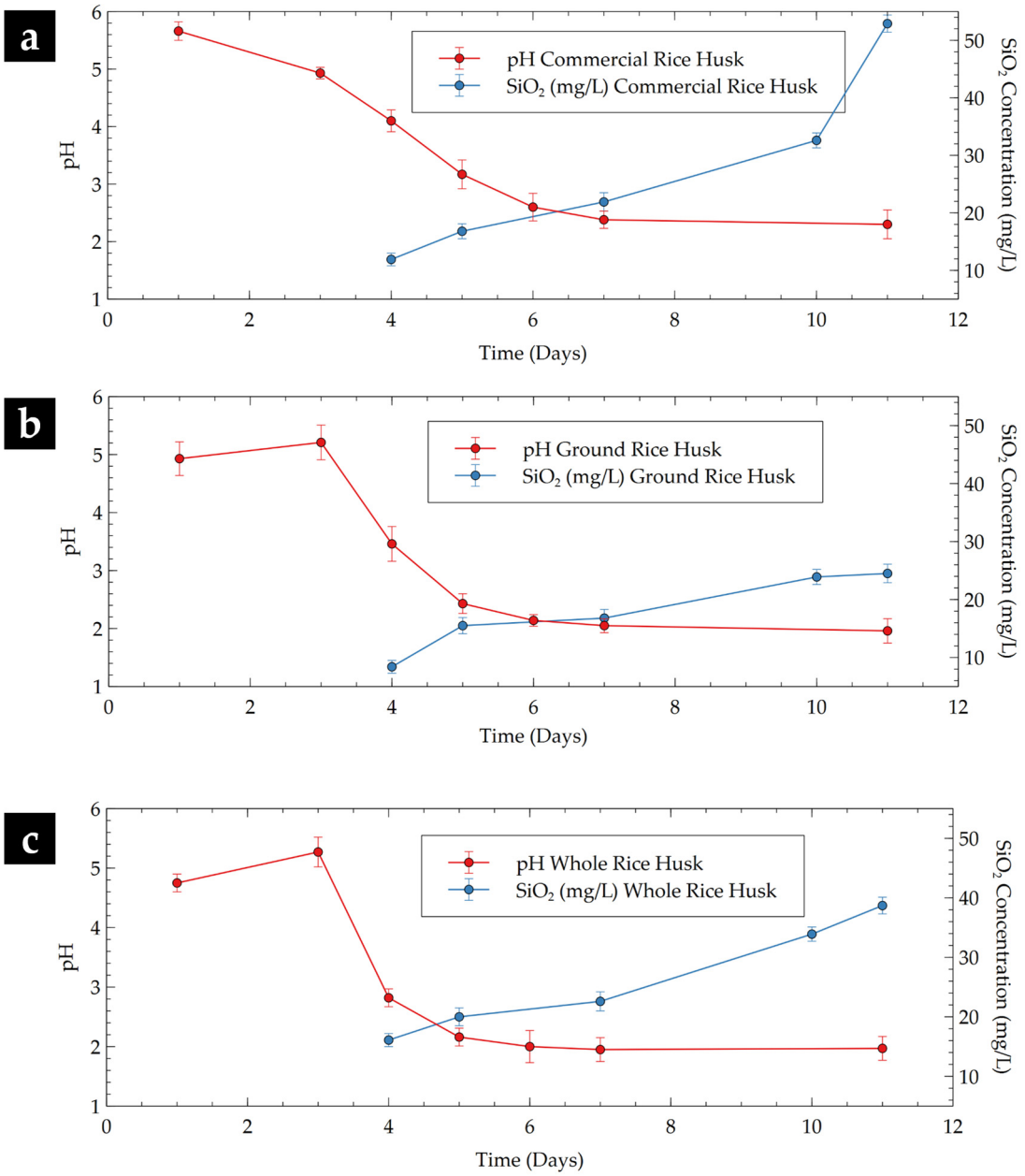


Figure 2. Monitoring of pH and soluble silica concentration during the bioleaching of different types of rice husk with *A. niger*. (**a**) commercial rice husk; (**b**) ground rice husk; (**c**) whole rice husk.

For whole rice husk (Figure 2c), a pH decrease to ~1.8 was observed between days 3 and 5, followed by a sustained increase in silica concentration, reaching values similar to those of commercial husk (~39 mg/L). Although particle size reduction is generally associated with increased surface area, the results obtained in this study indicate that this effect does not necessarily translate into improved silica release under biological conditions. This suggests that the structural integrity of the rice husk may play a key role in facilitating microbial interaction and silica transformation.

Several studies have reported the extraction of biogenic silica from rice husk using both chemical and biological approaches. Chemically assisted methods typically achieve high silica recoveries, often exceeding 80–90% through the use of strong alkaline or acidic treatments combined with elevated temperatures; however, these processes involve significant energy consumption and environmental burdens. In contrast, biologically mediated systems rely on the production of organic acids and operate under milder conditions,

where silica solubilization is driven by progressive acidification—commonly reaching pH values around 2–3—and microbial metabolism [5,7,19]. Recent studies have shown that bioleaching processes can effectively mobilize silica from rice husk, although extraction efficiencies are typically lower, often corresponding to partial solubilization in the range of tens of mg/L or limited percentage recovery, depending on process conditions [20,21].

In this study, maximum silica concentrations of approximately 52 mg/L for commercial rice husk and 39 mg/L for whole rice husk were achieved under ambient conditions without the use of calcination or external acid addition. These values are consistent with those reported for biologically assisted extraction systems, where silica release is typically moderate due to the gradual nature of microbial acidification and the structural complexity of lignocellulosic matrices [7,8,19]. Furthermore, the observed differences between substrates suggest that structural accessibility and particle refinement play a critical role in enhancing silica recovery, as reductions in particle size and increased surface area have been shown to significantly improve extraction performance [21].

Therefore, while the absolute silica recovery remains lower than that of conventional chemical routes, the proposed approach offers clear advantages in terms of environmental sustainability, reduced chemical input, and process simplicity. These findings align with recent literature emphasizing biologically driven silica extraction as a low-energy and environmentally friendly alternative for the valorization of rice husk and similar agroindustrial residues [5,19–21].

The observed relationship between medium acidification and silica release confirms the central role of *A. niger* metabolic activity in the bioleaching process. This mechanism is consistent with reports on biotransformation of siliceous materials, where the accumulation of organic acids generates a low-pH environment that promotes the cleavage of Si–O–Si bonds and silica solubilization [7,22].

The results suggest that the process involves an initial solubilization of silica followed by the formation of nanoscale silica-based structures within the system. This behavior may be associated with biologically mediated processes such as biomineralization, reprecipitation, or structural reorganization influenced by microbial activity and extracellular compounds. However, further studies would be required to elucidate the exact formation mechanism.

Regarding the apparent paradox of analyzing dissolved silicon dioxide in the solid state, it is important to clarify that two complementary analytical strategies were applied to different fractions of the fermentation system. UV–Vis spectrophotometry was performed on the filtered liquid fraction (supernatant), where solubilized silicic acid species and colloidal silica nanoparticles remain in suspension. In contrast, FTIR and FE-SEM analyses were carried out on the solid fraction recovered after fermentation, which corresponds to the partially transformed rice husk matrix bearing newly deposited nanostructures. This dual-fraction approach is necessary because silica simultaneously exists in soluble form in the liquid phase and as solid nanostructures reorganized onto or within the plant biomass matrix. As for the mechanism of particle reorganization from dissolved to solid state, the following hypothesis is proposed: as *Aspergillus niger* progressively acidifies the medium through organic acid production, Si–O–Si bonds in the amorphous silica matrix are cleaved, releasing monomeric silicic acid [$Si(OH)_4$] into solution. Once the local concentration of silicic acid exceeds the solubility threshold (approximately 100–200 mg/L at neutral-to-acidic pH), spontaneous polycondensation reactions occur, generating oligomeric silica clusters that grow into nanoscale particles through an Ostwald-ripening-like mechanism. Concurrently, the extracellular proteins, glycoproteins, and polysaccharides secreted by *A. niger* during fermentation are known to stabilize growing silica nuclei, acting as organic templates that direct particle assembly and prevent uncontrolled aggregation—a

mechanism analogous to biological silicification in diatoms and silicifying organisms [7,8]. Heterogeneous nucleation on the residual husk surface further promotes re-deposition of silica as nanoscale deposits embedded in the lignocellulosic matrix, which explains the morphological features observed by FE-SEM. This biologically modulated, two-stage solubilization–re-precipitation mechanism is consistent with the composite nature of the recovered material and with biomineralization processes reported for other fungal–mineral systems [7].

Although milling increases the initial rate of acidification, whole and commercial husk achieved higher final silica concentrations, suggesting that structural and compositional factors of the plant matrix influence silica availability. It is noteworthy that, according to Mirmohamadsadeghi et al. [5], the action of organic acids such as acetic, citric, and oxalic acids, also present in fungal fermentation, can be used as a pretreatment to remove metallic ions through cation exchange [6,23], thereby improving silica purity and achieving quality levels comparable to those obtained using mineral acids.

These results, in addition to highlighting the influence of particle size, emphasize the importance of substrate composition and structure in the overall efficiency of bioleaching. This opens the possibility of combining chemical and biological pretreatment strategies to optimize both silica extraction and the quality of the material obtained.

Although the silica recovery yield obtained in this study remains modest, the results demonstrate the feasibility of a biologically driven extraction pathway, which can be further enhanced through process optimization and scale-up strategies.

3.3. Characterization of the Obtained Silica-Containing Nanostructures

The silica-containing nanostructures generated through biosynthesis with *Aspergillus niger* were characterized using UV–Vis spectrophotometry, Fourier-transform infrared spectroscopy (FTIR), and field-emission scanning electron microscopy (FE-SEM). These analyses enabled the evaluation of their optical, chemical, and morphological properties, as well as comparison with nanosilica synthesized by other methods reported in the literature.

3.3.1. UV–Vis Spectrophotometry

The UV–Vis spectra exhibited absorption features consistent with silica-based structures, although contributions from organic compounds present in the system cannot be excluded. Figure 3 presents the UV–Vis absorption spectrum obtained after 11 days of biosynthesis from commercial rice husk.

The spectral profile shows intense absorption in the deep ultraviolet region (200–350 nm), with a maximum absorbance exceeding 3.5 units. This behavior is commonly associated with electronic transitions related to Si–O–Si bonds in amorphous silica networks [24]. However, it should be noted that the UV–Vis response in such systems may also be influenced by light scattering effects, particle size distribution, and the presence of residual organic components.

The absence of significant absorption features in the visible region (400–700 nm) indicates a predominantly UV-active material. Nevertheless, this observation should not be interpreted as definitive evidence of high optical purity, since low concentrations of organic or inorganic species may not produce distinct absorption bands in this region.

Compared with the data reported by Biradar et al. [22], who observed a maximum absorption around 297 nm for chemically synthesized nanosilica, the spectrum obtained in this study shows a globally similar trend, although with a smoother and less structured profile. These differences are expected and can be attributed to the biological synthesis route, which operates under mild conditions and leads to materials with higher structural heterogeneity and possible incorporation of organic residues. Additionally, UV–Vis spectra

are sensitive to particle size, aggregation state, and matrix composition; therefore, exact spectral matching with literature data is not expected in heterogeneous biogenic systems.

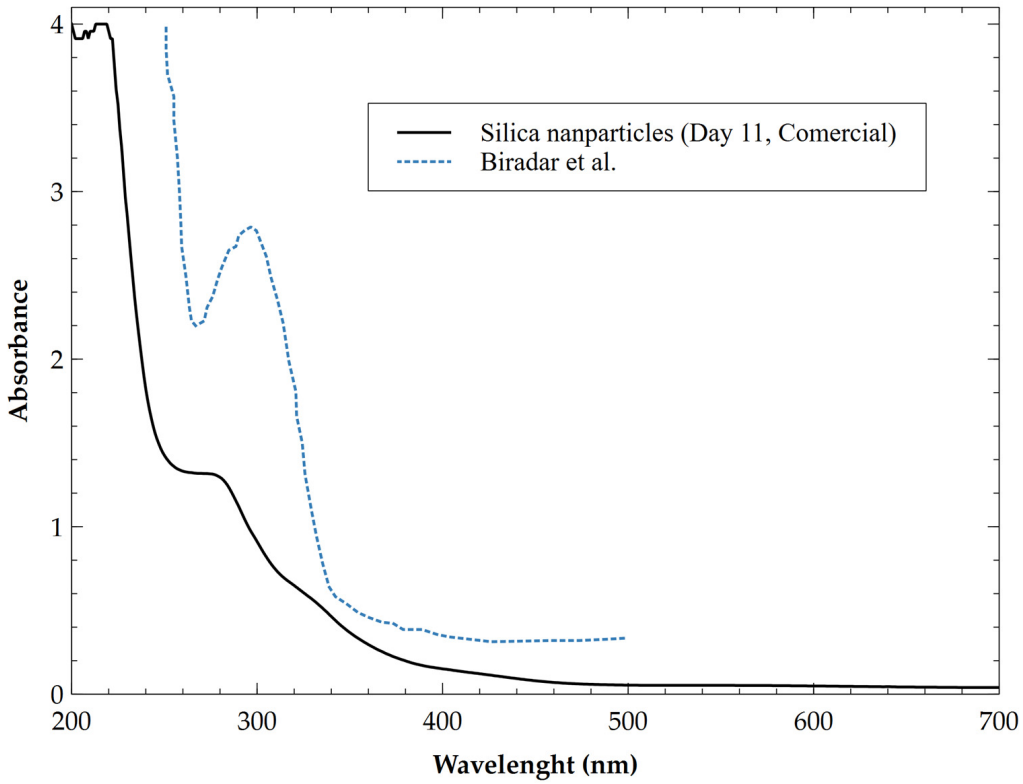


Figure 3. UV–Vis spectrum of silica nanoparticles obtained from commercial rice husk (CRH) on day 11 of biosynthesis (solid black line), compared with the results reported by Biradar et al. [22] (blue dashed line).

From the absorption edge, located around 230 nm, the optical band gap was estimated using the relation Eg = 1240/λ, yielding an approximate value of 5.39 eV. This value falls within the range typically reported for silica-based amorphous materials [25], although it should be interpreted cautiously due to the simplified nature of the estimation and the complex composition of the analyzed system.

The high band gap energy is consistent with the dielectric character of silica and its limited absorption in the visible region [26]. These findings suggest that the material retains key optical features associated with silica-based structures, supporting the potential of the proposed biotechnological route as an alternative for producing silica-containing materials with functional optical properties.

3.3.2. Fourier-Transform Infrared Spectroscopy (FTIR) Analysis

Figure 4 shows the FTIR spectrum of silica-containing nanostructures synthesized from rice husk through *Aspergillus niger*-assisted biosynthesis. The analysis was performed in the range of 4000 to 400 cm^{-1} and allowed the identification of functional groups present on the surface of the material, providing direct evidence of the chemical composition of the obtained nanoparticles [27].

The FTIR spectra revealed characteristic bands associated with Si–O–Si and Si–OH groups, indicating the presence of silica within the analyzed material, despite the coexistence of organic components from the biological matrix [28].

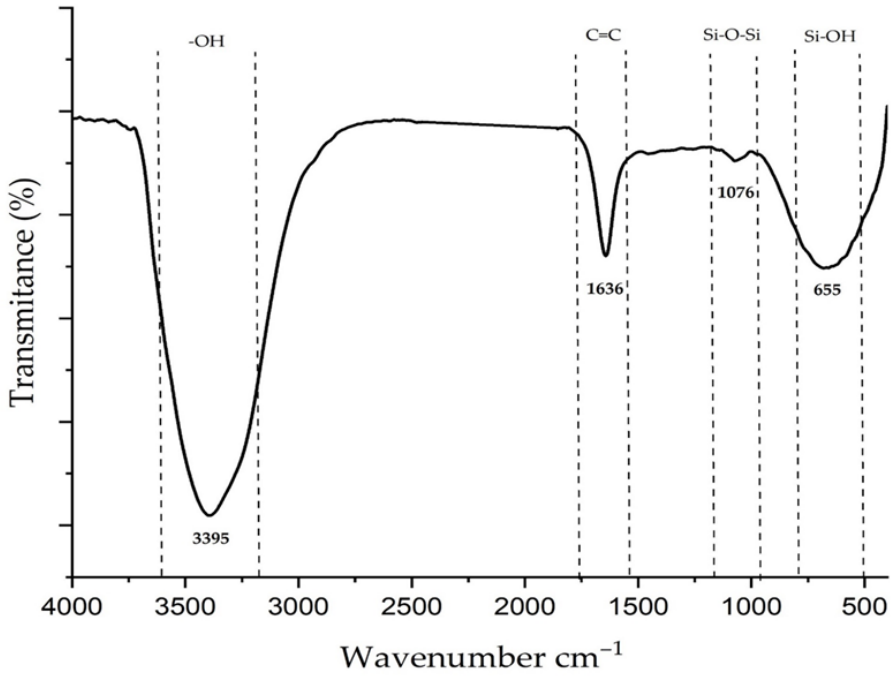


Figure 4. FTIR spectrum obtained from commercial rice husk (CRH) in the range of 400–4000 cm^{-1}.

In Figure 4, broad and prominent band centered at 3395 cm^{-1} was observed, corresponding to O–H stretching vibrations, typically associated with hydroxyl groups (–OH) from adsorbed water or surface silanols (Si–OH) [29]. This signal indicates a highly hydroxylated surface, a characteristic feature of amorphous silica and of great importance for its colloidal dispersion and subsequent chemical functionalization.

In the mid-region, a band at 1636 cm^{-1} was identified, attributed to bending vibrations of molecular water or possible C=C bonds derived from residual organic compounds originating from the culture medium. Although not predominant, its presence suggests that part of the organic content was not completely removed during the purification process [29], which is common in biogenic synthesis of silica nanoparticles [3].

The most significant peak was located at 1076 cm^{-1}, corresponding to the asymmetric stretching vibration of the Si–O–Si bond. This is the most distinctive band of silicon dioxide-based materials and confirms the formation of a siloxane network characteristic of amorphous silica [19]. Additionally, a band at 655 cm^{-1} was identified, likely corresponding to bending vibrations of Si–OH groups or deformation modes of the siloxane backbone [19]. This further supports the presence of hydroxylated functional groups on the surface, which are relevant for applications in catalysis and controlled release systems.

The obtained results are consistent with those reported by Rahman et al. [21], who demonstrated that the physicochemical and optical properties of nanosilica are strongly influenced by particle size. Although particle size was not controlled through directed synthesis in the present study, the FTIR data, together with the UV–Vis results, suggest that the nanoparticles fall within the sub-100 nm range, where surface effects and structural defects dominate their behavior.

Specifically, Rahman et al. [21] associated the band at 1076 cm^{-1} with the angular structure of the siloxane network. A shift of this band toward lower wavenumbers correlates with a decrease in the Si–O–Si bond angle as particle size decreases. In this study, the intensity and position of the peak suggest an amorphous structure rich in distorted bonds, consistent with small nanoparticles containing a higher proportion of coordinatively unsaturated atoms.

The intense vibration at 3395 cm^{-1}, related to –OH groups, is consistent with Rahman et al. [21], who observed that silanol group concentration increases significantly as particle size decreases, thereby enhancing surface reactivity. This property is highly desirable in applications requiring functional group anchoring, biomolecule immobilization, or heterogeneous catalysis.

From an optical perspective, Ilka et al. [26] also reported that smaller nanoparticles exhibit a higher density of surface defects, such as E′ centers and oxygen vacancies, reflected in increased UV absorbance. In the present study, the high absorbance in the 200–250 nm range and the estimated band gap value of 5.39 eV (Section 3.3.1) are consistent with the presence of such defects and a surface rich in silanol groups, suggesting favorable performance in applications such as UV-protective coatings and photonic substrates.

Rahman et al. [21] further discussed that, at the nanoscale, a reduction in the number of silanol groups per unit surface area (αOH) may occur due to the incomplete siloxane network in small particles. This phenomenon could explain the moderate band at 655 cm^{-1} observed in this study, attributed to vibrations of isolated or defective Si–OH groups, possibly located at edges or corners of the nanoparticles.

3.3.3. FE-SEM Microscopy Analysis

The FE-SEM images showed nanoscale structures associated with the solid matrix, which, together with spectroscopic evidence, suggest the presence of silica-based nanostructures within a heterogeneous system. The FE-SEM images presented in Figure 5 reveal significant morphological changes in the rice husk after the biological treatment. The untreated sample (Figure 5b) exhibits a relatively smooth and organized surface, characteristic of lignocellulosic materials. In contrast, the treated samples (Figure 5a,c) show a markedly rough and heterogeneous surface, with the presence of particulate deposits distributed across the matrix.

At higher magnification (80,000×), nanoscale spherical to sub-spherical structures and agglomerated features can be observed. These morphologies are consistent with those reported for silica-based nanostructures, although they are embedded within a complex matrix derived from the original biomass and microbial activity [27].

It is important to note that FE-SEM provides morphological information only and does not allow direct chemical identification of the observed structures. Therefore, the features observed are interpreted as nanoscale deposits formed during the process, which are consistent with silica-containing structures when considered together with the spectroscopic results.

The particle size distribution (Figure 5d) indicates that a significant fraction of the observed structures falls within the nanoscale range, supporting the formation of nanostructured material during the biosynthesis process. With a mode of 41–51 nm and most particles concentrated in the 41–61 nm interval, according to the histogram generated from image analysis (ImageJ Fiji, version 1.54f; National Institutes of Health, Bethesda, MD, USA).

In comparison with Zielonka et al. [2], who reported particles with pyramidal (~400 nm), cubic (~85 nm), and spherical (~3–24 nm) geometries, the nanoparticles obtained in this study exhibit a more homogeneous and predominantly spherical morphology. These differences may arise from both the fungal species employed (*A. niger* vs. *A. parasiticus*) and the absence of aggressive thermal treatments. Such homogeneity may represent an advantage in applications requiring uniformity, such as optical coatings, controlled release systems, or colloidal formulations.

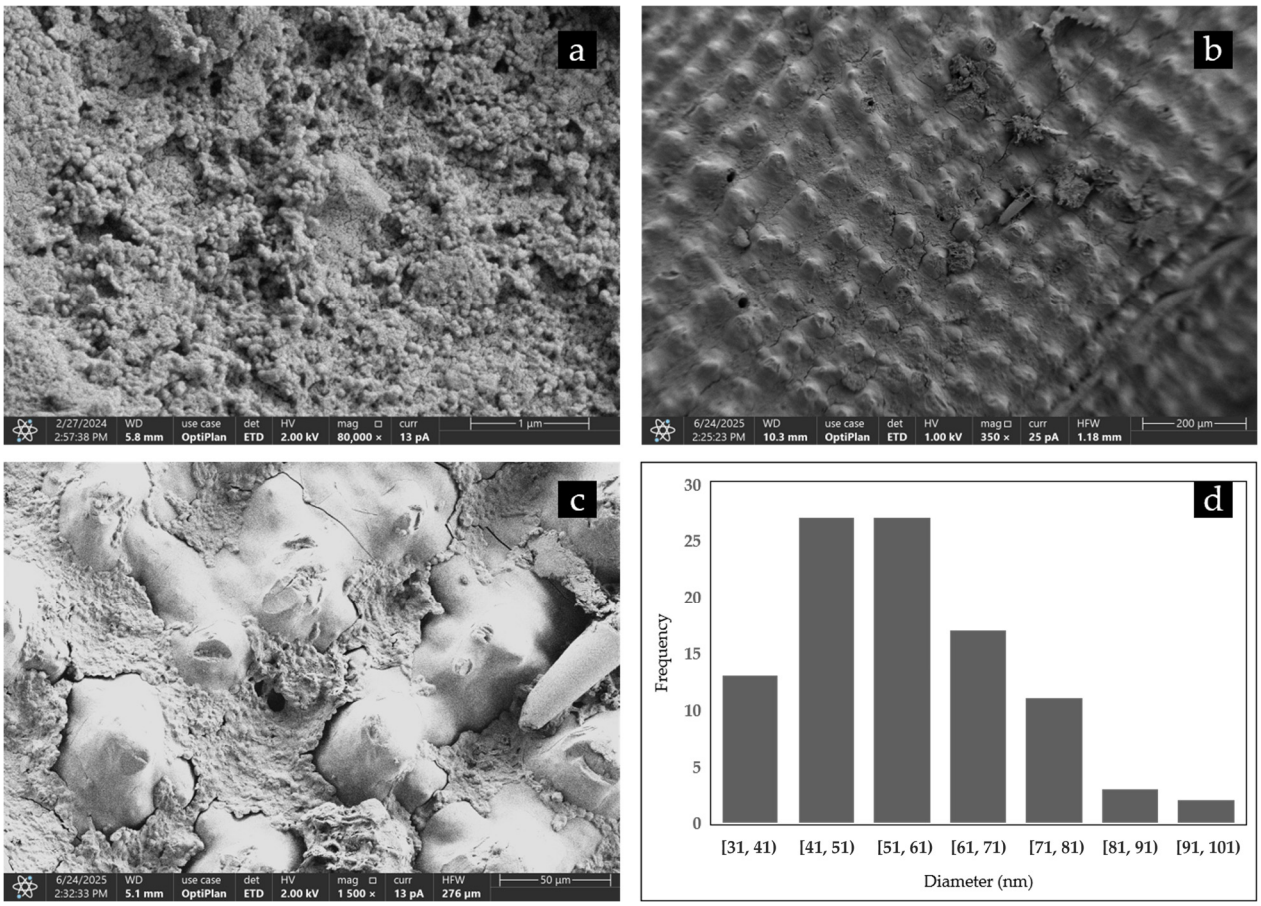


Figure 5. FE-SEM micrographs of commercial rice husk (CRH) after biosynthesis with *Aspergillus niger*. (**a**) High-magnification view (80,000×, 2.00 kV) showing spherical to sub-spherical nanoparticles with a tendency toward agglomeration. (**b**) General view (350×, 1.00 kV) illustrating the surface texture of the substrate and particle distribution within the matrix. (**c**) Intermediate detail (1500×, 2.00 kV) displaying porous domains and amorphous silica deposits associated with the plant framework. (**d**) Nanoparticle size distribution obtained by image analysis (ImageJ Fiji), with a range of 31–100 nm and a mode between 41 and 51 nm.

A relevant point of comparison is the recent study by Kaur et al. [29], conducted under the supervision of Ruchi Agrawal, which reported the synthesis of biogenic silica nanoparticles from rice straw and its lignin-rich bioethanol residue (LRBR) using cell-free extract of the bacterium *Bacillus amyloliquefaciens*. While both studies exploit biological routes to recover silica from agroindustrial residues, several fundamental differences distinguish our approach. First, the substrate differs: Kaur et al. [29] used rice straw and a pre-processed bioethanol residue rich in lignin, whereas the present work directly employs intact rice husk in its native forms (commercial, whole, and ground) without any prior chemical or thermal pretreatment. Second, the microorganism and mechanism differ substantially: the former study applied bacterial cell-free extract supplemented with 1% HCl (*v*/*v*) to promote nucleation, which introduces an exogenous acid; our study relies entirely on whole-culture fungal fermentation by *A. niger*, where organic acids, extracellular enzymes (including exo-polygalacturonase, endo-xylanase, and manganese peroxidase), and other metabolites are produced in situ, without any added mineral acid. Third, the analytical framework differs: Kaur et al. [29] quantified elemental silicon by atomic absorption spectroscopy (AAS) and characterized hydrodynamic particle size by dynamic light scattering, whereas our study integrates UV–Vis spectrophotometry of the liquid fraction, FTIR, and FE-SEM–EDS of the solid fraction, providing complementary structural and morphological evidence.

Fourth, our work explicitly operates without calcination, whereas Kaur et al. [29] did not address the calcination issue. Despite the general thematic similarity, these methodological differences make the two studies complementary rather than duplicative, and they address distinct niches within the broader field of biologically mediated silica recovery from rice-based residues. In this regard, the present study constitutes, to the best of our knowledge, the first report of direct whole-culture fungal bioleaching applied to uncalcined, native rice husk for composite silica nanostructure production.

Elemental analysis by EDS performed in representative areas confirmed the predominant presence of Si and O, along with minor signals of C (likely associated with residual organic matter or the carbon support) and Au (originating from the conductive coating), as shown in Figure 6. This composition supports the identification of amorphous silicon dioxide.

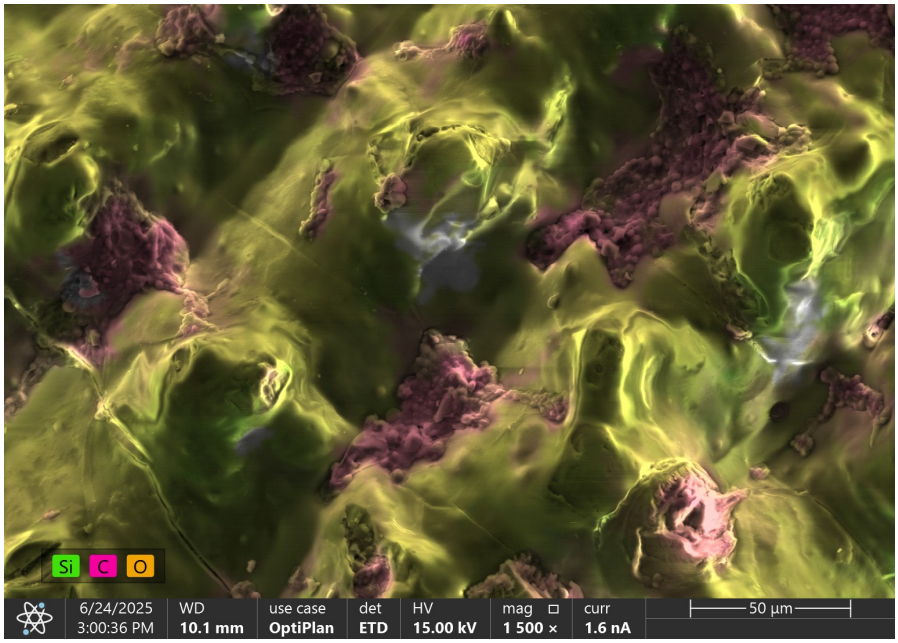


Figure 6. EDS elemental mapping of rice husk, showing the spatial distribution of Si, O, and C across the lignocellulosic matrix. The heterogeneous silica-rich regions are highlighted, confirming the presence and localization of silicon within the substrate (mag. 1500×; scale bar = 50 µm).

The sustainability of the proposed approach warrants a nuanced discussion. We acknowledge that the sucrose concentration used (140 g/L) is high and could be perceived as an economic limitation. However, this concentration was adopted from established citric acid fermentation media optimized for maximal metabolic activity of *A. niger* [11,12], and represents a starting point for proof-of-concept rather than an optimized industrial formulation. Future work can explore substantially reduced sucrose concentrations or the use of low-cost alternative carbon sources (e.g., molasses, lignocellulosic hydrolysates) without compromising biological activity. It is also important to note that the fermentation broth produced in this process contains a rich array of value-added metabolites beyond citric acid, including extracellular enzymes (pectinases, hemicellulases, ligninases), gluconic acid, and oxalic acid, all of which contribute to the silica solubilization process through distinct and synergistic mechanisms [6,7]. Unlike a simple acid treatment with pure citric acid, the whole-culture fungal fermentation generates a biologically regulated, self-buffering, multi-component system that avoids the external dosing of mineral acids and the associated handling, neutralization, and waste disposal costs. The sustainability of the process should therefore be assessed holistically: in terms of energy input (ambient temperature, no calcination), chemical inputs (no added mineral acids), waste reduction

(valorization of agroindustrial residue), and potential for process integration within biorefinery frameworks. Yield improvement through design-of-experiment optimization of sucrose loading, pulp density, pH control, and fermentation time represents a clear and achievable pathway for future development, and does not undermine the fundamental scientific novelty demonstrated in this proof-of-concept study.

Taken together, the UV–Vis, FTIR, and FE-SEM analyses provide complementary evidence supporting the formation of silica-containing nanostructures during the biological treatment of rice husk with *Aspergillus niger*. The UV–Vis spectra revealed a strong absorption response in the ultraviolet region for the liquid-phase fraction, indicating the presence of silica-related species in solution or colloidal form. FTIR analysis of the recovered solid showed characteristic vibrational bands associated with Si–O–Si and Si–OH groups, confirming the presence of silica within the material, although contributions from organic components were also observed. In parallel, FE-SEM images revealed nanoscale spherical to sub-spherical structures distributed over the lignocellulosic matrix, consistent with the formation of silica-based deposits under biologically mediated conditions.

These results indicate that the process involves not only the solubilization of silica from rice husk, but also its subsequent reorganization or deposition into nanoscale structures within a heterogeneous biological system. While the combined evidence supports the formation of silica-containing nanostructures, further purification and advanced compositional analyses would be required to fully determine the chemical purity and formation mechanism of the material.

4. Conclusions

The biologically mediated treatment of rice husk using *Aspergillus niger* enabled the formation of composite silica-based amorphous nanostructures under ambient conditions, without the need for calcination or the external addition of strong mineral acids. Kinetic monitoring revealed that medium acidification, from an initial pH of 5.5 to values close to 2.0, played a key role in silica solubilization, consistent with the in situ production of organic acids during microbial metabolism. Commercial rice husk (CRH) reached maximum concentrations of approximately 52 mg/L, whereas whole husk (WM) and ground husk (GM) reached approximately 39 mg/L and 30 mg/L, respectively, indicating that substrate structure influences process efficiency alongside particle size. These findings further suggest that particle size reduction is not necessarily advantageous under the evaluated biological conditions, and that preserving the structural integrity of the rice husk may enhance microbial interaction and silica transformation.

These findings confirm that the proposed biotechnological route is technically effective and environmentally advantageous compared to conventional chemical methods, particularly due to its operation under ambient conditions without calcination or external acid addition. Unlike traditional approaches that rely on high energy input and aggressive reagents, this study demonstrates that composite silica nanostructures can be generated through biologically induced acidification, providing a low-impact alternative for silica recovery. Moreover, this work provides experimental evidence that substrate structure, rather than particle size reduction alone, plays a critical role in biologically mediated silica transformation, offering new insights into process design for bioleaching systems. The results validate the potential of rice husk as a valorized agroindustrial resource within biorefinery schemes aligned with circular economy principles. The physicochemical properties of the obtained composite nanostructures—including their UV-active behavior, Si–O–Si surface chemistry, and nanoscale particle size—suggest potential suitability for future investigation in applications such as UV-protective coatings, heterogeneous catalysis supports, and

adsorption-based systems, subject to further purification, compositional characterization, and performance validation.

The proposed method demonstrates the feasibility of a biologically mediated route for silica recovery from rice husk, although further optimization is required to improve yield and process efficiency.

Author Contributions: Conceptualization, D.E.-D., S.G.-M., L.R.-C., M.R.-C. and C.O.-L.; validation, D.E.-D., S.G.-M., L.R.-C., M.R.-C. and C.O.-L.; formal analysis, D.E.-D., S.G.-M., L.R.-C., M.R.-C. and C.O.-L.; investigation, D.E.-D., S.G.-M., L.R.-C., M.R.-C. and C.O.-L.; resources, M.R.-C. and L.R.-C.; data curation, D.E.-D., S.G.-M., L.R.-C., M.R.-C. and C.O.-L.; writing—original draft preparation, D.E.-D., S.G.-M., L.R.-C., M.R.-C. and C.O.-L.; writing—review and editing, D.E.-D., S.G.-M., L.R.-C., M.R.-C. and C.O.-L.; visualization, D.E.-D., S.G.-M., L.R.-C., M.R.-C. and C.O.-L.; supervision, L.R.-C., M.R.-C. and C.O.-L.; funding acquisition, L.R.-C., M.R.-C. and C.O.-L. All authors have read and agreed to the published version of the manuscript.

Funding: The APC was funded by Universidad Pontificia Bolivariana.

Institutional Review Board Statement: Not applicable.

Informed Consent Statement: Not applicable.

Data Availability Statement: The original contributions presented in this study are included in the article. Further inquiries can be directed to the corresponding author.

Conflicts of Interest: The authors declare no conflicts of interest.

References

1. Mohamad Sopi, S.A.I.; Abu Hassan, M.H. A Review on the Extraction of Silica Nanoparticles from Poaceae Family via Sol-Gel. *Malays. J. Sci. Health Technol.* **2024**, *10*, 7–18. [CrossRef]
2. Zielonka, A.; Żymańczyk-Duda, E.; Brzezińska-Rodak, M.; Duda, M.; Grzesiak, J.; Klimek-Ochab, M. Nanosilica Synthesis Mediated by Aspergillus Parasiticus Strain. *Fungal Biol.* **2018**, *122*, 333–344. [CrossRef]
3. Ghorbani, F.; Sanati, A.M.; Maleki, M. Production of Silica Nanoparticles from Rice Husk as Agricultural Waste by Environmental Friendly Technique. *Environ. Stud. Persian Gulf* **2015**, *2*, 56–65.
4. Grand View Research. *NanoSilica Market Size Report, 2025–2033*; Grand View Research: San Francisco, CA, USA, 2024. Available online: https://www.grandviewresearch.com/industry-analysis/nanosilica-market (accessed on 12 February 2026).
5. Mirmohamadsadeghi, S.; Karimi, K. Recovery of Silica from Rice Straw and Husk. In *Current Developments in Biotechnology and Bioengineering*; Elsevier: Amsterdam, The Netherlands, 2020; pp. 411–433.
6. Rendón-Castrillón, L.; Ramírez-Carmona, M.; Ocampo-López, C.; Gómez-Arroyave, L. Bioleaching Techniques for Sustainable Recovery of Metals from Solid Matrices. *Sustainability* **2023**, *15*, 10222. [CrossRef]
7. Bansal, B.; Ahmad, A.; Sastry, M. Fungus-Mediated Biotransformation of Amorphous Silica in Rice Husk to Nanocrystalline Silica. *J. Am. Chem. Soc.* **2006**, *128*, 14059–14066. [CrossRef] [PubMed]
8. Pineda-Vásquez, T.G.; Casas-Botero, A.E.; Ramírez-Carmona, M.E.; Torres-Taborda, M.M.; Soares, C.H.L.; Hotza, D. Biogeneration of Silica Nanoparticles from Rice Husk Ash Using Fusarium Oxysporum in Two Different Growth Media. *Ind. Eng. Chem. Res.* **2014**, *53*, 6959–6965. [CrossRef]
9. Pineda, T.; Hotza, D.; Soares, C.H.L.; Casas, A.; Ramírez, M.; Cortés, V. Biotransformação Da Cinza Da Casca de Arroz Em Nanopartículas de Sílica Mediante Fusarium Oxysporum. *Rev. Matéria.* **2012**, *17*, 946–954. [CrossRef]
10. *ASTM E11-17*; Standard Specification for Woven Wire Test Sieve Cloth and Test Sieves. ASTM International: West Conshohocken, PA, USA, 2017. Available online: https://www.astm.org/e0011-17.html (accessed on 3 January 2026).
11. Papagianni, M. Advances in Citric Acid Fermentation by Aspergillus Niger: Biochemical Aspects, Membrane Transport and Modeling. *Biotechnol. Adv.* **2007**, *25*, 244–263. [CrossRef]
12. Kim, J.-W.; Barrington, S.; Sheppard, J.; Lee, B. Nutrient Optimization for the Production of Citric Acid by Aspergillus Niger NRRL 567 Grown on Peat Moss Enriched with Glucose. *Process Biochem.* **2006**, *41*, 1253–1260. [CrossRef]
13. *ASTM D859-16(2021)e1*; Standard Test Method for Silica in Water. ASTM International: West Conshohocken, PA, USA, 2021. Available online: https://www.astm.org/d0859-16r21e01.html (accessed on 3 January 2026).
14. Balakrishnan, V.; Ab Wab, H.A.; Abdul Razak, K.; Shamsuddin, S. In Vitro Evaluation of Cytotoxicity of Colloidal Amorphous Silica Nanoparticles Designed for Drug Delivery on Human Cell Lines. *J. Nanomater.* **2013**, *2013*, 729306. [CrossRef]
15. Buazar, F. Impact of Biocompatible Nanosilica on Green Stabilization of Subgrade Soil. *Sci. Rep.* **2019**, *9*, 15147. [CrossRef]

16. Venkatathri, N.; Nanjundan, S. Synthesis and Characterization of a Mesoporous Silica Microsphere from Polystyrene. *Mater. Chem. Phys.* **2009**, *113*, 933–936. [CrossRef]
17. Tiller, V.; Meyerhoff, J.; Sziele, D.; Schügerl, K.; Bellgardt, K.-H. Segregated Mathematical Model for the Fed-Batch Cultivation of a High-Producing Strain of Penicillium Chrysogenum. *J. Biotechnol.* **1994**, *34*, 119–131. [CrossRef]
18. Olawale, O.; Oyawale, F.A.; Makinde, O.W.; Ogundele, K.T. Effect of Oxalic Acid on Rice Husk. *Int. J. Appl. Sci. Eng. Res.* **2012**, *1*, 663–668. [CrossRef]
19. Rodier, L.; Savastano, H. Use of Glass Powder Residue for the Elaboration of Eco-Efficient Cementitious Materials. *J. Clean. Prod.* **2018**, *184*, 333–341. [CrossRef]
20. Ge, X.; Xie, J.; Song, X.; Cao, X.; Wang, Y.; Xu, Z.; Wang, Y.; Hou, X. Electrokinetic Remediation of Cadmium (Cd), Copper (Cu) and Nickel (Ni) Co-Contaminated Soil with Oxalic Acid, Acetic Acid or Citric Acid as the Catholyte. *Int. J. Electrochem. Sci.* **2022**, *17*, 220444. [CrossRef]
21. Rahman, I.A.; Vejayakumaran, P.; Sipaut, C.S.; Ismail, J.; Chee, C.K. Size-Dependent Physicochemical and Optical Properties of Silica Nanoparticles. *Mater. Chem. Phys.* **2009**, *114*, 328–332. [CrossRef]
22. Biradar, A.I.; Sarvalkar, P.D.; Teli, S.B.; Pawar, C.A.; Patil, P.S.; Prasad, N.R. Photocatalytic Degradation of Dyes Using One-Step Synthesized Silica Nanoparticles. *Mater. Today Proc.* **2021**, *43*, 2832–2838. [CrossRef]
23. Zavodinsky, V.G.; Kuyanov, I.A.; Zavodinskaya, O.M. Atomic and Electronic Structures of Nanometer Sized Silica Particles. *J. Non. Cryst. Solids* **1999**, *243*, 123–136. [CrossRef]
24. Nor, R.M.; Halim, S.N.M.; Taib, M.F.M.; Abd-Rahman, M.K. First Principles Investigation on the Structural, Electronic and Optical Properties of Amorphous Silica Glass. *Solid State Phenom.* **2017**, *268*, 92–96. [CrossRef]
25. Tran, T.N.; Pham, T.V.A.; Phung Le, M.L.; Thoa Nguyen, T.P.; Tran, V.M. Synthesis of Amorphous Silica and Sulfonic Acid Functionalized Silica Used as Reinforced Phase for Polymer Electrolyte Membrane. *Adv. Nat. Sci. Nanosci. Nanotechnol.* **2013**, *4*, 045007. [CrossRef]
26. Ilka, M.; Bera, S.; Kwon, S.-H. Influence of Surface Defects and Size on Photochemical Properties of SnO_2 Nanoparticles. *Materials* **2018**, *11*, 904. [CrossRef] [PubMed]
27. Babu, R.H.; Yugandhar, P.; Savithramma, N. Synthesis, Characterization and Antimicrobial Studies of Bio Silica Nanoparticles Prepared from *Cynodon dactylon* L.: A Green Approach. *Bull. Mater. Sci.* **2018**, *41*, 65. [CrossRef]
28. Dubey, R.S.; Rajesh, Y.B.R.D.; More, M.A. Synthesis and Characterization of SiO_2 Nanoparticles via Sol-Gel Method for Industrial Applications. *Mater. Today Proc.* **2015**, *2*, 3575–3579. [CrossRef]
29. Kaur, P.; Singh, S.; Sharma, N.; Agrawal, R. Filling in the Gaps in Second-Generation Biorefineries: Evaluating Rice Straw and Its Bioethanol Residue for the Production of Biogenic Silica Nanoparticles. *Nanotechnol. Environ. Eng.* **2024**, *9*, 67–76. [CrossRef]

Disclaimer/Publisher's Note: The statements, opinions and data contained in all publications are solely those of the individual author(s) and contributor(s) and not of MDPI and/or the editor(s). MDPI and/or the editor(s) disclaim responsibility for any injury to people or property resulting from any ideas, methods, instructions or products referred to in the content.